

# A Framework for IoT-Enabled Virtual Emotion Detection in Advanced Smart Cities

Hyunbum Kim, Jalel Ben-Othman, Sungrae Cho, and Lynda Mokdad

## ABSTRACT

A barrier coverage has been studied widely because it provides guaranteed detection of mobile objects after a barrier is constructed. Also, many researchers have investigated the recognition of human emotion by facial expression and human gesture or motion with possible high accuracy. In particular, thanks to recent remarkable advancements of technology, it is possible to recognize human emotion by wireless signal. In this article, we introduce a new emotion-detectable framework in advanced smart cities with a concept of barrier coverage in IoT-enabled environments. The proposed framework allows IoT devices to create a virtual emotion barrier, called a *VEmoBar*, which is able to sense human emotion through a wireless signal and its reflection. Also, we define a problem whose goal is to form a specific number of *VEmoBars* which returns a maximum cumulative accuracy. To solve the problem, we propose a novel approach as well as a system initialization and then evaluate them through extensive simulations with various scenarios. Moreover, we discuss future issues and challenges toward future promising smart cities based on this virtual emotion framework.

## INTRODUCTION

Emotion is a unique feature of humans because emotion can be created only by humans. This notable feature allows us to distinguish humans from machines. Also, it is a fact that computing machines or systems can offer useful services to humans by recognizing their emotions with possible computational models [1].

For the recognition of human emotion, there exist several research branches. First, the emotion can be derived from audio and visual information such as voice, facial expression, gesture or motion recognition using cameras [2, 3]. Also, it is possible that emotion can be measured by physiological signals including heart rate, body temperature through wearable devices and body sensors [4, 5]. Recently, researchers developed an important emotion recognition scheme using wireless signals reflected by the human body [6, 7]. So, with a reduction of limitation and implementation requirements, the technique using wireless signals allows the system to infer a person's emotions from a wireless signal and its reflection. In particular, the approach based on wireless signals has clear advantages when compared with other approaches [8]. For example, emotion recogni-

tion using wireless signals has a better coverage than cameras because wireless signals can penetrate walls or other physical objects. However, cameras may have limited angles and need additional requirements such as a good luminosity. Moreover, wireless signal based solutions can reduce privacy issues since cameras may cause unwanted capture including sensitive information of people such as a user's face.

It has been known that the Internet of Things (IoT) [9, 10] should be one of the promising concepts toward proper emotion-based services. Then, it is highly appropriate that we accomplish emotion recognition using wireless signals in IoT environments for private areas and public areas consisting of various IoT devices. After an IoT device transmits a wireless signal to a human and receives heartbeat and respiration signals through its reflection, it is then possible to derive the emotions of the person by their feature extractions [6, 7]. Furthermore, if an IoT-enabled system can detect specific groups with serious emotions such as extreme anger, fury and can also monitor specific regions with those emergent situations continuously by IoT devices equipped with wireless signals, it follows that the system can give people rapid and custom-made services based on the detection of emotions. Figure 1 depicts possible emotion-based applications by wireless signal. Figure 1a depicts emotion recognition and derivation processes by wireless signal at private areas such as private home and smart car. After the emotion recognition, it is possible to provide custom-made services to the person. Also, Fig. 1b represents possible applications of emotion-based services at public areas after agreement of people is satisfied for installing emotion-detectable IoT device to public areas. For example, if the system perceives serious emotions such as extreme fury or fear at public transportation areas, it is able to give the reinforced security service by patrolling the specific area.

It is anticipated that those emotion-based services for citizens will contribute to the realization of successful advanced smart cities. In particular, when we want to sense the emotions of people, a concept of barrier coverage [11] should be a good solution for this purpose. If we construct a barrier by a set of devices within a given area, then any movement or penetration of objects between one region and another is guaranteed to be sensed by at least one device within the built barrier. But, because wireless signals may return different emotion accuracy depending on the dis-

tance between device and object, we should take into account this issue critically to pursue highly accurate emotion detection by IoT-enabled barriers.

Based on the above observation, we introduce a framework for virtual emotion detection toward future advanced smart cities. Then, our contributions can be summarized as follows. We design a framework that is able to provide virtual emotion detection by barriers consisting of IoT devices. To the best of our knowledge, this is the first approach to introduce the concept of *virtual emotion barrier* fitting with an IoT environment where the detected information not only can be kept as manipulatable data in the system but also can be transmitted to other devices of entities.

Different from [12], we formally define a problem, *k-MaxCAEmo*, whose objective is to form *k* number of *virtual emotion barriers* in the given region such that the cumulative accuracy of those barriers is maximized. To solve the problem, we then propose the *Max-k-Cumulative-Accuracy-Selection* approach that returns *k* number of *virtual emotion barriers* with the maximum cumulative accuracy for emotion detection.

Also, the performance of the proposed scheme is evaluated through extensive simulations with various scenarios. Furthermore, we discuss research challenges and future issues that can be studied critically based on the proposed framework.

## A FRAMEWORK FOR IoT-BASED VIRTUAL EMOTION DETECTION

In this section, we present the proposed framework for IoT-based virtual emotion detection in advanced smart cities. First, we explain assumptions and settings that are considered in our system. Then, the concept of virtual emotion barrier is introduced and the *k-MaxCAEmo* problem is defined.

### ASSUMPTIONS AND SYSTEM SETTINGS

Now we describe the assumptions and settings that are considered in the proposed system:

- For emotion categorization, the proposed system seeks to recognize four emotion types including joy, pleasure, sadness, and anger.
- Heterogeneous IoT devices with different maximum signal ranges are located at the square-shaped area.
- Each IoT device is able to transmit wireless signals to a person within the signal range and it also has procedures to derive and detect four emotion types through wireless signal reflection [6, 7].
- Emotion detection accuracy based on wireless signals can be different depending on the distance between the person and the IoT device. Also, the system has pre-defined accuracy rate information according to the wireless signal range of the device.
- The recognized emotion information can be stored as data or a kind of multimedia such as voice and video in the system and it also can be sent to other entities [13]. Also, the information can be utilized for numerous applications such as Artificial Intelligence (AI) services [14].

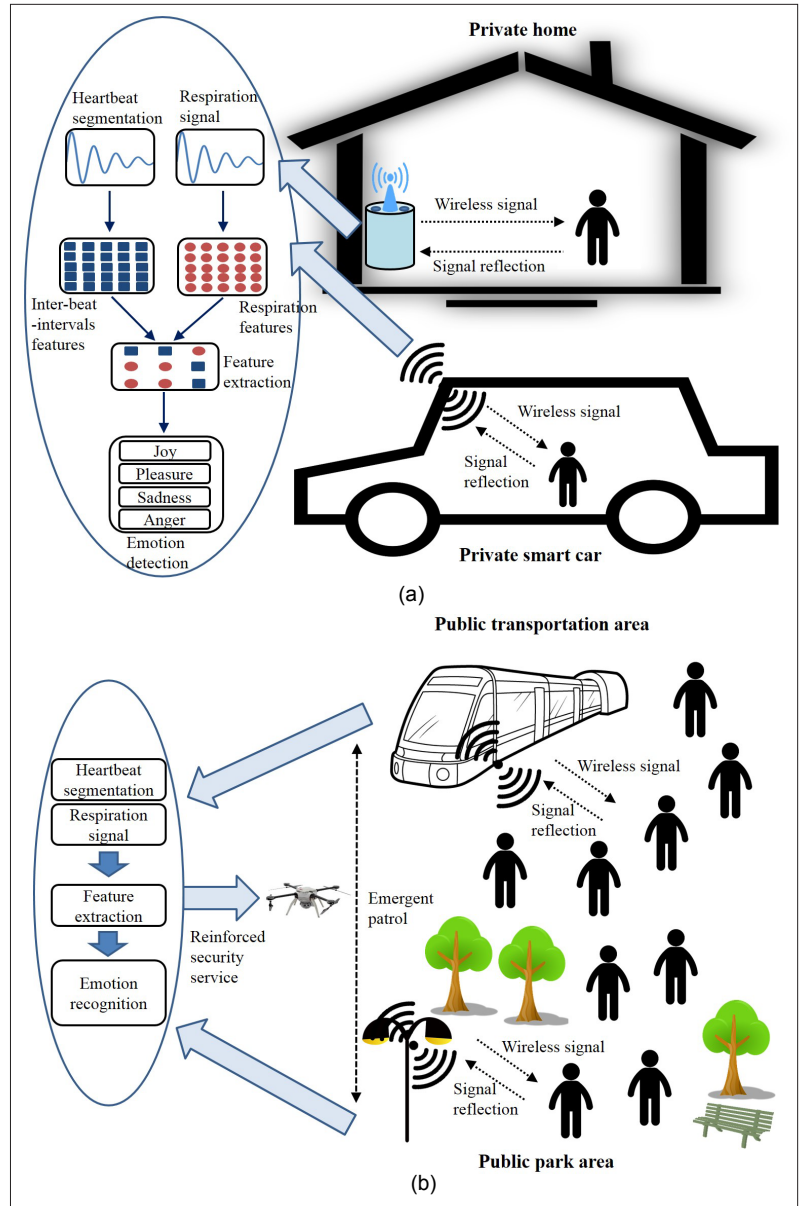


FIGURE 1. Possible emotion-based applications by wireless signal at private areas and public areas: a) an example of emotion detection at private areas; b) an example of emotion detection at public areas.

### VIRTUAL EMOTION BARRIER AND ITS CONSTRUCTION

As one of the promising research branches, emotion recognition has attracted much interest from researchers in both academic institutions and key industries because detecting possibly correct emotions of humans allows systems to achieve custom-made services for a specific person or group. Also, it is noted that emotion recognition by wireless signal [6] has several advantages of increased coverage and reduced privacy when it is compared with other emotion recognition schemes based on audio/video information and physiological signals. In particular, if it is possible to detect and derive a precise human emotion in an IoT environment, it motivates the system to carry out useful AI-enabled services to citizens, which will be one of the goals in future IoT-based smart cities.

We now define the concept of virtual emotion which is utilized in the proposed framework.

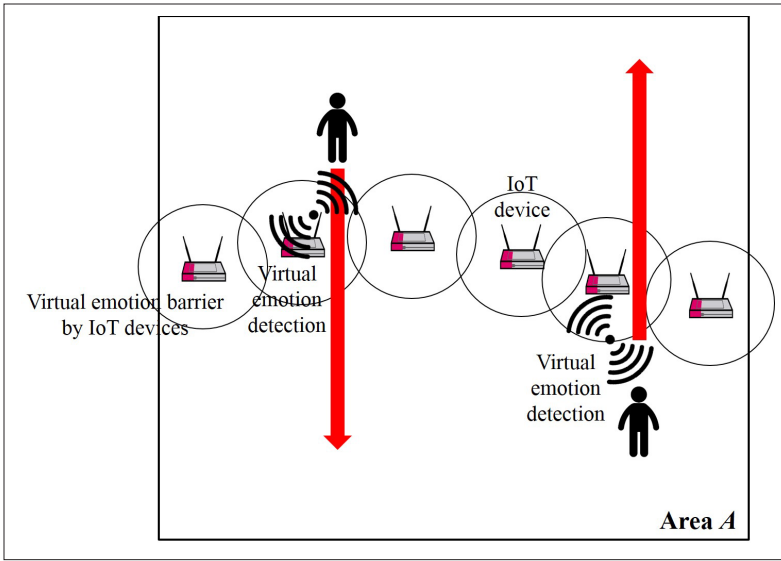


FIGURE 2. An example of emotion detection by the constructed virtual emotion barrier.

**Virtual Emotion:** Given that an IoT device is equipped with wireless signal, each IoT device is able to transmit the wireless signal and to receive its reflection so that it can derive the emotions of humans through pre-installed processing units of heartbeat segmentation, respiration signal and feature extraction going through a wireless signal's reflection. Then, the derived emotion is defined as a *virtual emotion* that can be kept as manipulatable data as well as be sent to other devices in AI-enabled applications.

Also, it has been known that as the distance between a person and an IoT device for wireless signal increases, the accuracy of emotion recognition decreases [6]. For example, an emotion recognition accuracy with distance 10 m between the IoT device and the human is higher than the accuracy with a distance of 20 m. Hence, the accuracy issue should be addressed critically in emotion-related applications and our system also reflects upon the derivation of the accurate *virtual emotion*.

Based on this observation, we introduce a new form of barrier, *virtual emotion barrier* which is called *VEmoBar*, in order to guarantee the detection of emotions within a given area where numerous IoT devices are involved. The proposed system aims at providing a person or people with appropriate AI-enabled services with a highly expected matching probability according to the detected emotion of the person by IoT devices. The proposed barrier concept is defined as follows.

**Virtual Emotion Barrier (VEmoBar):** It is given that a set of IoT devices are positioned at a square-shaped area where IoT devices can sense and derive virtual emotions using a wireless signal and its reflection. A *virtual emotion barrier*, called *VEmoBar*, is a barrier that detects the emotion of humans who move from one side to another side.

Figure 2 depicts an example of virtual emotion detection. Given area A, a virtual emotion barrier can be generated by the connected set of heterogeneous IoT devices where each device has its own maximum wireless signal range and

two devices can be connected if the signals by two devices meet at each other when their maximum signal ranges are used. Then, as can be seen in Fig. 2, the organized virtual emotion barrier is aware of virtual emotion of any person who is moving from one side to another (i.e., from top to bottom or from bottom to top.)

### PROBLEM DEFINITION

In the proposed system, an institutive goal is to detect virtual emotions by the constructed *VEmoBar* of IoT devices with possible high accuracy. In [11], the authors concentrated on finding the maximum number of barriers because the life-time of the barrier system can be prolonged by applying sleep-wakeup scheduling alternately. For example, while one barrier is active, other barriers are in sleep mode to save battery life. After that, the mode of the current activated barrier is transformed into the sleep mode and then some barrier with sleep mode previously is activated. Such a sleep-wakeup scheduling is executed using a set of alternating barriers. Different from [11], we propose the virtual emotion barrier consisting of heterogeneous IoT devices where each IoT device has different maximum wireless signal ranges. Because wireless signals may cause different virtual emotion detection accuracy depending on the distance between the device and the object, we consider the issue and also introduce the *VEmoBar* with a concept of cumulative accuracy so that the human emotion is guaranteed to be detected by at least  $k$  number of IoT devices with possible high cumulative accuracy. Now, we formally define the  $k$ -MaxCAEmo problem that is to be solved in the proposed framework.

**$k$ -MaxCAEmo:** Suppose that a set of  $n$  number of IoT devices  $T$  with a list of different signal ranges  $R$  are located at the area A. Also, the system has pre-determined emotion detection accuracy by the wireless signal range and the distance between a device and a person. Then, the  $k$ -MaxCAEmo problem is to maximize the cumulative accuracy of emotion detection with the construction of  $k$  number of *VEmoBar* such that the cumulative accuracy is calculated by multiplying every estimated accuracy between IoT devices within  $k$  number of *VEmoBar*.

That is, the objective function of the  $k$ -MaxCAEmo problem is to maximize the cumulative accuracy of *VEmoBar*, referred to as  $C_A$ , such that  $k$  number of *VEmoBar* consisting of  $vb_1, vb_2, \dots, vb_k$  are constructed. After forming  $k$  number of *VEmoBar*, each *VEmoBar*  $vb_m$  has its detection accuracy which is referred as  $A_{vb_1}, A_{vb_2}, \dots, A_{vb_k}$  where  $1 \leq m \leq k$ . It follows that the final  $C_A = A_{vb_1} \cdot A_{vb_2} \cdot \dots \cdot A_{vb_k}$ . Then, the objective function of the  $k$ -MaxCAEmo problem is to:

$$\text{Maximize } C_A \quad (1)$$

Figure 3 shows examples of building  $k$  number of *VEmoBar* with possibly high cumulative accuracy. Suppose that a set of IoT devices  $T = \{t_1, t_2, \dots, t_n\}$  are positioned within the area A and we have a pre-defined accuracy rate information depending on the distance. In Fig. 3a, there exist three *VEmoBar*:  $vb_1, vb_2, vb_3$ .  $vb_1$  is composed of  $t_1, t_2, t_3, t_4, t_5, t_6$ ;  $vb_2$  includes  $t_7, t_8, t_9, t_{10}, t_{11}$ ;  $vb_3$  consists of  $t_{12}, t_{13}, t_{14}, t_{15}, t_{16}, t_{17}$ . Note that the



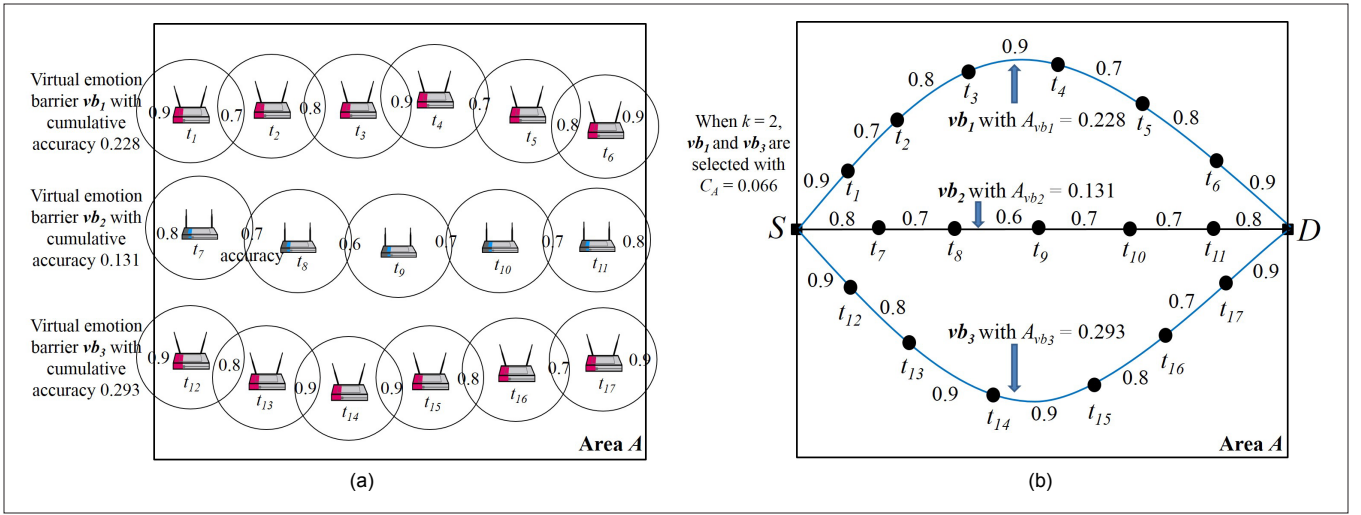


FIGURE 3. An example of virtual emotion barrier construction with a consideration of cumulative accuracy when  $k = 2$ : a) an example of virtual emotion barrier construction with cumulative accuracy; b) an example of a graph expression with  $k = 2$ .

accuracy is assigned for every pair of neighbor devices. Then, we mark the accuracy between two devices  $t_i$  and  $t_j$  as  $a_{t_i, t_j}$ . For example, in  $vb_1$ , the accuracy value 0.7 is assigned between  $t_1$  and  $t_2$  depending on the wireless signal range and it follows that  $a_{t_1, t_2} = 0.7$ . If so,  $vb_1$ 's detection accuracy  $A_{vb_1}$  can be calculated as  $a_{t_1, t_2} \cdot a_{t_2, t_3} \cdot a_{t_3, t_4} \cdot a_{t_4, t_5} \cdot a_{t_5, t_6}$  which returns 0.228 in Fig. 3a. Similarly, the detection accuracy of  $vb_2$  and  $vb_3$  can be estimated. So, as can be seen in Fig. 3a,  $A_{vb_2}$  is 0.131 and  $A_{vb_3}$  is 0.293, respectively. On the other hand, Fig. 3b represents a graph expression of  $vb_1$ ,  $vb_2$ ,  $vb_3$  from Fig. 3a. From source  $S$  to destination  $D$ , we can make three  $VEmoBar$ ,  $vb_1$ ,  $vb_2$ ,  $vb_3$ . In order to solve the  $k$ -MaxCAEmo problem with  $k = 2$ , we should choose  $vb_1$  and  $vb_3$  because  $vb_2$ 's detection accuracy is low. Hence, for the  $k$ -MaxCAEmo problem, we can calculate the cumulative accuracy  $C_A = A_{vb_1} \cdot A_{vb_3}$  which returns 0.066 in Fig. 3b. In summary, the cumulative accuracy  $C_A$  is maximized such that  $k$  number of  $VEmoBar$  is formed to guarantee that the emotion of a person moving from one region to another is detected by at least  $k$  devices with possible high accuracy.

## PROPOSED APPROACH

In this section, we address the proposed approach to solve the  $k$ -MaxCAEmo problem. In our system, the Max-k-Cumulative-Accuracy-Selection approach is implemented after the Initialization procedure.

### INITIALIZATION

To construct  $k$  number of  $VEmoBar$  using IoT devices equipped with wireless signals, we first perform *Initialization* that returns the initial IoT graph  $\mathcal{G}_T = (V(\mathcal{G}_T), E(\mathcal{G}_T))$  including the determined accuracy among IoT devices. Then, the steps of *Initialization* are described as follows:

- Verify a square-shaped IoT area  $A$  and a set of IoT devices  $T = \{t_1, t_2, \dots, t_n\}$  including a list of their different maximum signal ranges  $R = \{r_{t_1}, r_{t_2}, \dots, r_{t_n}\}$ .
- Generate virtual source  $S$  and destination  $D$  which can be considered as two opposite sides depending on the detection direction.

- Using  $R$ , each IoT device checks neighbor devices. For example, two devices  $t_i$  and  $t_j$  become a neighbor relation at each other and can be connected with each other if the Euclidean distance  $Euc(t_i, t_j)$  between two devices is less than equal to the sum of their maximum signal ranges  $r_{t_i} + r_{t_j}$ .
  - Using the pre-defined accuracy reference  $Y$  depending on wireless signal ranges, each device  $t_i$  has a node accuracy value  $a_{t_i}$ . Then, the edge accuracy value  $a_{t_i, t_j}$  is assigned if  $t_i$  and  $t_j$  have neighbor relation where  $a_{t_i, t_j}$  is decided as the minimum value of  $a_{t_i}$  and  $a_{t_j}$  so that  $a_{t_i, t_j} = \min(a_{t_i}, a_{t_j})$ .
  - Then, the initial IoT graph  $\mathcal{G}_T = (V(\mathcal{G}_T), E(\mathcal{G}_T))$  is created. It follows that the set of IoT devices including  $S$  and  $D$  is matched as the set of vertices  $V(\mathcal{G}_T)$ .  $S$  and  $D$  are added to  $V(\mathcal{G}_T)$ . Also, every neighbor relation  $e(t_i, t_j)$  with accuracy value is transformed into  $E(\mathcal{G}_T)$ .
- The pseudocode of *Initialization* is described in Algorithm 1 in more detail.

### MAX-K-CUMULATIVE-ACCURACY-SELECTION APPROACH

After *initialization* procedure, the system has the initial IoT graph  $\mathcal{G}_T = (V(\mathcal{G}_T), E(\mathcal{G}_T))$ . Based on the graph, we propose the *Max-k-Cumulative-Accuracy-Selection* approach that generates  $k$  number of  $VEmoBar$  with maximum cumulative accuracy so as to solve the  $k$ -MaxCAEmo problem. Then, the *Max-k-Cumulative-Accuracy-Selection* approach is performed by the below steps:

- Create the set of  $VEmoBar$  as  $B$  and set  $B$  as empty initially.
- Generate status graph  $\mathcal{G}_T' = (V(\mathcal{G}_T'), E(\mathcal{G}_T'))$  which is derived from  $\mathcal{G}_T = (V(\mathcal{G}_T), E(\mathcal{G}_T))$ . It follows that  $\mathcal{G}_T$  is converted into  $\mathcal{G}_T'$  on condition that every vertex  $i \in V(\mathcal{G}_T')$  divides into two vertices  $i_{in}$  and  $i_{out}$  and we consider a directional edge  $i_{in} \rightarrow i_{out}$ . Also, if nodes  $i$  and  $j$  have an edge in  $\mathcal{G}_T$ , a directional edge is expressed as  $j_{out} \rightarrow i_{in}$  in  $\mathcal{G}_T'$  for each incoming edge from  $j$  to  $i$  in  $\mathcal{G}_T$ . Similarly, for each outgoing edge from  $i$  to  $j$  in  $\mathcal{G}_T$ ,  $\mathcal{G}_T'$  has a directional edge  $i_{out} \rightarrow j_{in}$ .
- For  $\mathcal{G}_T' = (V(\mathcal{G}_T'), E(\mathcal{G}_T'))$ , we apply the Edmonds-Karp algorithm [15] to discover the

Inputs:  $A, T, R, n, Y$ , Output:  $\mathcal{G}_T = (V(\mathcal{G}_T), E(\mathcal{G}_T))$

- 1: set  $\mathcal{G}_T = (V(\mathcal{G}_T), E(\mathcal{G}_T)) = \emptyset$ ;
- 2: verify target area  $A$  and its detection direction;
- 3: create source  $S$  and destination  $D$ ;
- 4: add  $S$  and  $D$  to  $V(\mathcal{G}_T)$ ;
- 5: for  $i = 1$  to  $n$  do
- 6:   set  $V(\mathcal{G}_T) \leftarrow V(\mathcal{G}_T) \cup t_i$ ;
- 7: end for
- 8: for  $i = 0$  to  $n - 1$  do
- 9:   for  $j = i + 1$  to  $n$  do
- 10:     if  $\text{Euc}(i, j) \leq r_{t_i} + r_{t_j}$  then
- 11:       set  $E(\mathcal{G}_T) \leftarrow E(\mathcal{G}_T) \cup e(t_i, t_j)$  with the edge accuracy  $a_{t_i, t_j}$  from  $Y$  where  $a_{t_i, t_j} = \min(a_{t_i}, a_{t_j})$ ;
- 12:     end if
- 13:   end for
- 14: end for
- 15: return  $\mathcal{G}_T = (V(\mathcal{G}_T), E(\mathcal{G}_T))$

ALGORITHM 1. Initialization.

Inputs:  $\mathcal{G}_T, k$ , Output:  $C_A$  or *false*.

- 1: set  $C_A = 0$ ;
- 2: set  $B = \emptyset$ ;
- 3: set  $P = \emptyset$ ;
- 4: set  $\mathcal{G}_T' = \emptyset$ ;
- 5: convert  $\mathcal{G}_T$  into  $\mathcal{G}_T'$  such that every vertex  $i$  has two vertices  $i_{in}$  and  $i_{out}$  and there exist directional edges  $i_{in} \rightarrow i_{out}$ ,  $j_{out} \rightarrow i_{in}$ ,  $i_{out} \rightarrow j_{in}$  where  $i, j \in V(\mathcal{G}_T'), i \neq j$ ;
- 6: while  $\mathcal{G}_T' \neq \emptyset$  do
- 7:   search for the independence path in  $\mathcal{G}_T'$  from  $S$  to  $D$ ;
- 8:   if an independence path  $P_c$  is found then
- 9:     calculate  $A_{P_c}$ ;
- 10:     add  $P_c$  to the candidate set  $P$ ;
- 11:   else
- 12:     break;
- 13:   end if
- 14: end while
- 15: if  $|P| < k$  then
- 16:   return *false*;
- 17: else
- 18:   select  $k$  candidates with the highest cumulative accuracy;
- 19:   add those  $k$  candidates to  $B$ . Then,  $B = \{B_1, B_2, \dots, B_k\}$ ;
- 20:   calculate  $C_A = A_{B_1} \times A_{B_2} \times \dots \times A_{B_k}$ ;
- 21:   return  $C_A$ ;
- 22: end if

 ALGORITHM 2. Max- $k$ -Cumulative-Accuracy-Selection.

maximum number of independent paths (or node-disjoint paths). Then, the found  $m$  number of independent paths become a potential set of candidates where  $P = \{P_1, P_2, \dots, P_m\}$ . If the set size of  $P$  is less than  $k$ , return false. Otherwise, continue the below steps.

- For each candidate  $P_c$  where  $P_c \in P$ , verify its constructing devices and their edge accuracy values from  $\mathcal{G}_T$ . Then, estimate the cumulative accuracy values  $A_{P_c}$  of each candidate in  $P$ .
- From  $P$ , choose  $k$  number of candidates with the highest cumulative accuracy.
- Add the selected candidates to  $B$ . So,  $B = \{B_1, B_2, \dots, B_k\}$ .
- For updated barriers, calculate  $C_A = A_{B_1} \times A_{B_2} \times \dots \times A_{B_k}$  and the  $C_A$  is returned as the ultimate output.

Also, the pseudocode of the Max- $k$ -Cumulative-Accuracy-Selection approach is represented in Algorithm 2 in more detail.

In this section, we evaluate the performance of the proposed schemes. Our simulations cover various square-shaped regions such as width  $500 \times$  height  $200$ ,  $500 \times 300$ ,  $500 \times 400$ ,  $500 \times 500$ ,  $500 \times 600$ ,  $500 \times 700$ ,  $500 \times 800$ ,  $500 \times 900$ ,  $500 \times 1000$ , respectively. Also, the number of IoT devices ranges from 50 to 200 and those IoT devices are deployed randomly within the square-shaped area. Also, we consider heterogeneous IoT devices so that each IoT device has different maximum wireless signal ranges. In the experiments, the maximum wireless signal range of devices ranges from 55 to 80. It follows that each device has different wireless signal ranges whose maximum bound is from 55 to 80 when the system assigns the signal range to each device randomly. By Algorithm 2, our simulation returns  $C_A$  as the successful final result or returns *false* if the set size of  $P$  is less than  $k$ . It is noted that each experiment in the utilized result graph represents the average value of  $C_A$  for 100 successful cases with different graph sets. Based on those settings, we first performed the *Initialization* procedure and then *Max- $k$ -Cumulative-Accuracy-Selection* is implemented using  $\mathcal{G}_T$  which is the result of Initialization. Also, when  $k$  number of VEMoBar are generated within the given square-shaped area, we applied various  $k$  values as  $k = 1, 2, 3$ , respectively.

Largely, our experiments are classified with two scenarios. In the first scenario of simulations, we consider a different number of devices and various signal ranges of devices in the area with width  $500 \times$  height  $500$ . Figure 4a shows the result when the number of devices is 50; Fig. 4b describes the result when the number of devices is 100; Fig. 4c shows the performance of the proposed scheme when the number of devices is 150; 200 devices are utilized in Fig. 4d. As can be seen in Fig. 4, the value of cumulative accuracy  $C_A$  decreases as the maximum signal range of devices increases. In particular, when the system has the bigger value of  $k$ , the proposed approach returns the smaller values of  $C_A$  as a whole. For instance, we are able to check that the case of  $k = 2$  returns the smaller value of  $C_A$  than the case of  $k = 1$  and the case of  $k = 3$  also has the smaller  $C_A$  than the cases of  $k = 1$  and  $k = 2$ .

For the second group of experiments, we also deliberate on different sizes of square-shaped areas and the number of devices is 100 and the wireless signal ranges of devices are ranging from 55 to 80. Figures 5a and 5b show the results for the areas with width  $500 \times$  height  $200$  and  $500 \times 300$ ; Figs. 5c and 5d describe the results for the regions with  $500 \times 400$  and  $500 \times 600$ ; Fig. 5g depicts the result using the area with  $500 \times 700$ ; Fig. 5f depicts the result using  $500 \times 800$  as the area. Furthermore, Fig. 5g shows the result of  $C_A$  within  $500 \times 900$ ; Fig. 5h represents the result for the area of  $500 \times 1000$ . Similar to the results in the first group of experiments, through the second group of simulations, it is confirmed that as the maximum signal range of devices is increasing, the value of cumulative accuracy  $C_A$  is decreasing. On the other hand, if the system uses the bigger value of  $k$ , the Max- $k$ -Cumulative-Accuracy-Selection algorithm still gets the smaller

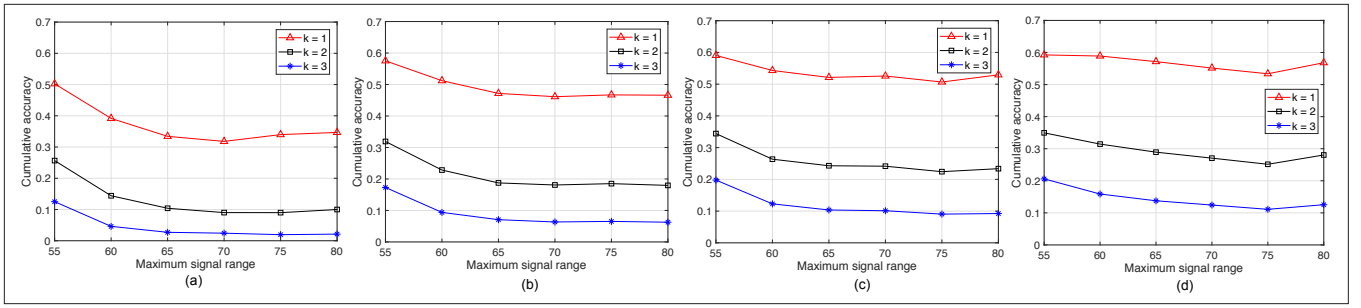


FIGURE 4. Comparison for cumulative accuracy  $C_A$  by different  $k$  with various number of devices in the area  $500 \times 500$ : a)  $n = 50$  in  $500 \times 500$  area; b)  $n = 100$  in  $500 \times 500$  area; c)  $n = 150$  in  $500 \times 500$  area; d)  $n = 200$  in  $500 \times 500$  area.

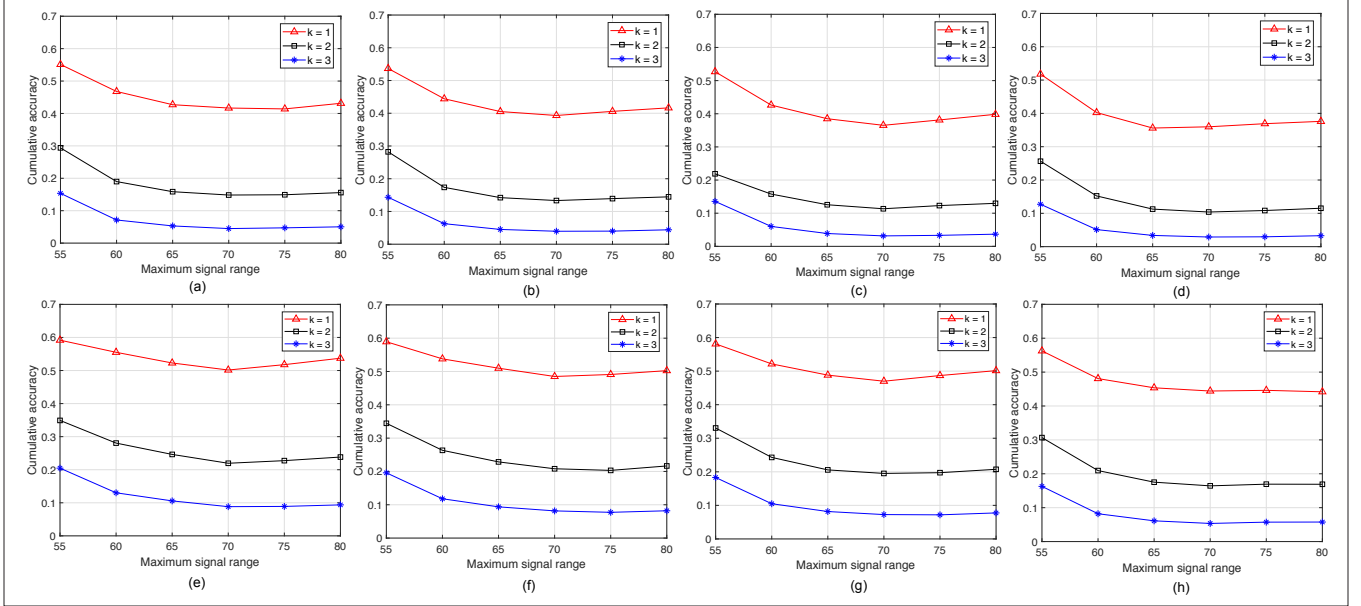


FIGURE 5. Comparison for cumulative accuracy  $C_A$  by different  $k$  with  $n = 100$  in various area sizes: a)  $n = 100$  in  $500 \times 200$  area; b)  $n = 100$  in  $500 \times 300$  area; c)  $n = 100$  in  $500 \times 400$  area; d)  $n = 100$  in  $500 \times 600$  area; e)  $n = 100$  in  $500 \times 700$  area; f)  $n = 100$  in  $500 \times 800$  area; g)  $n = 100$  in  $500 \times 900$  area; h)  $n = 100$  in  $500 \times 1000$  area.

results for  $C_A$  within the second group of results. For example, we could verify that the case of  $k = 3$  returns the smaller results of CA than other cases  $k = 1$  and  $k = 2$ , respectively.

## RESEARCH CHALLENGES AND FUTURE WORKS

In this section, we discuss research challenges and future issues based on the proposed infrastructure.

### VARIATION FOR DETECTABLE TYPES OF EMOTION

The proposed system assumed that IoT devices are able to detect four emotion types including joy, pleasure, sadness, and anger. Depending on the requirement and the objective of the pursuing system, it is appropriate to develop a light system that is capable of detecting a specific emotion type only. For example, each IoT in the light system only focuses on detection of only one emotion type and we can design the system whose goal is to derive only one or a few types of emotions to seek the lightness of the system instead of deriving all emotion types. In addition, finding the optimal number of devices and their strategic formations maintaining the same number of *VEmoBar* in the given area can be one of the issues to aim at system efficiency with a maximum life.

### CONSTRUCTION OF VIRTUAL EMOTION BARRIER WITH

## GUARANTEED DELAY BOUND

Let us remember that by generating  $k$  number of *VEmoBar* in the proposed framework, the emotions of a moving person in the area can be detected by at least  $k$  devices in the constructed *VEmoBar* with possible high cumulative accuracy. However, depending on the formed shapes of  $k$  number of *VEmoBar*, there may be a relatively long delay between two *VEmoBar* to recognize the emotion of a mobile person passing through the area if the distance between two devices is far such that two devices are covered by different *VEmoBar*. Therefore, this can be one of the research challenges. We plan to devise a model that is capable of providing the guaranteed delay bound among every *VEmoBar* in the given area.

### EXPANDED SUPPORTABLE AREAS WITH VARIOUS SHAPES AND OBSTACLES

The proposed infrastructure requires the construction of *VEmoBar* within only square-shaped areas. To fulfill various mission objectives and requirements, it is highly reasonable to build  $k$  number of *VEmoBar* which is workable for various types of regions including convex polygon, convex hull, and so on. Hence, it is necessary to develop novel methods to be able to create *VEmoBar* correctly for various shapes of areas. In partucluar, those

Providing services based on human emotion by IoT devices should be indispensable toward a successful realization of future advanced smart cities. To secure a bridgehead for those emotion-based services in IoT and AI-enabled smart cities, we designed a framework that is capable of detecting virtual emotion by VEmoBar that is composed of heterogeneous IoT devices.

areas may include several obstacles with a view of a practical scenario. Then, when we have multiple obstacles in the given areas, a successful construction of VEmoBar with high accuracy and a development of solid strategies can be another branch of future research challenges.

## CONCLUDING REMARKS

Providing services based on human emotion by IoT devices should be indispensable toward a successful realization of future advanced smart cities. To secure a bridgehead for those emotion-based services in IoT and AI-enabled smart cities, we designed a framework that is capable of detecting virtual emotion by VEmoBar that is composed of heterogeneous IoT devices. To the best of our knowledge, this is the first work to introduce the concept of *virtual emotion barrier* fitting with IoT environments where the detected information can be kept as manipulatable data in the proposed infrastructure as well as be transmitted to other entities. Also, we defined the *k-MaxCAEmo* problem whose objective is to create *k* number of VEmoBar such that the cumulative accuracy of those barriers is maximized. To solve the problem, we proposed the *Max-k-Cumulative-Accuracy-Selection* approach based on the *Initialization* procedure. Then, we analyzed the performance of the proposed scheme through extensive simulations with various settings and scenarios. Moreover, we discussed possible research challenges and presented our future plans to deal with those critical issues.

## REFERENCES

- [1] J. Gratch and S. Marsella, "Evaluating a Computational Model of Emotion," *J. Autonomous Agents and Multiagent Systems*, vol. 11, no. 1, July, 2005, pp. 23–43.
- [2] Z. Zeng et al., "A Survey of Affect Recognition Methods: Audio, Visual, and Spontaneous Expressions," *IEEE Trans. Machine Intelligence*, vol. 31, no. 1, Jan., 2009, pp. 39–58.
- [3] S. E. Kahou et al., "Emonets: Multimodal Deep Learning Approaches for Emotion Recognition in Video," *J. Multimodal User Interfaces*, vol. 10, no. 1, June, 2016, pp. 99–111.
- [4] F. Agraftoti, D. Hatzinakos, and A. K. Anderson, "ECG Pattern Analysis for Emotion Detection," *IEEE Trans. Affective Computing*, vol. 3, no. 1, Jan. 2012, pp. 102–15.
- [5] D. S. Quintana et al., "Heart Rate Variability is Associated with Emotion Recognition: Direct Evidence for a Relationship Between the Autonomic Nervous System and Social Cognition," *Int'l. J. Psychophysiology*, vol. 86, no. 2, Nov., 2012, pp. 168–72.
- [6] M. Zhao, F. Adib, and D. Katabi, "Emotion Recognition Using Wireless Signals," *Proc. ACM MobiCom*, Oct. 2016, pp. 95–108.
- [7] M. Zhao, F. Adib, and D. Katabi, "Emotion Recognition Using Wireless Signals," *Communications of the ACM*, vol. 61, no. 9, 2018, pp. 91–100.
- [8] W. Wang et al., "Device-Free Human Activity Recognition Using Commercial Wifi Devices," *IEEE JSAC*, vol. 35, no. 5, May 2017, pp. 1118–31.
- [9] B. Fekade et al., "Probabilistic Recovery of Incomplete Sensed Data in IoT," *IEEE Internet of Things J.*, vol. 5, no. 4, Aug., 2018, pp. 2282–92.
- [10] B. Kang, D. Kim, and H. Choo, "Internet of Everything: A Large-Scale Autonomic IoT Gateway," *IEEE Trans. Multi-Scale Computing Systems*, vol. 3, no. 3, July, 2017, pp. 206–14.

- [11] S. Kumar, T.H. Lai, and A. Arora, "Barrier Coverage with Wireless Sensors," *Proc. 11th Annual Int'l Conf. Mobile Computing and Networking (MobiCom)*, August, 2005, pp. 284–98.
- [12] H. Kim et al., "On Virtual Emotion Barrier in Internet of Things," *Proc. IEEE Int'l. Conf. Communications (ICC)*, May 2018, pp. 1–6.
- [13] M. Chen, P. Zhou, and G. Fortino, "Emotion Communication System," *IEEE Access*, vol. 5, Dec. 2016, pp. 326–37.
- [14] M. Frutos-Pascual and B. G. Zapirain, "Review of the Use of AI Techniques in Serious Games: Decision Making and Machine Learning," *IEEE Trans. Computational Intelligence and AI in Games*, vol. 9, no. 2, June 2017, pp. 133–52.
- [15] J. Edmonds and R. M. Karp, "Theoretical Improvements in Algorithmic Efficiency for Network Flow Problems," *J. ACM*, vol. 19, no. 2, April 1972, pp. 248–64.

## BIOGRAPHIES

HYUNBUM KIM received his Ph.D. degree in computer science from the University of Texas at Dallas, USA, in 2013. He is currently an assistant professor in the Department of Computer Science at the University of North Carolina at Wilmington, USA. His research interests include algorithm design and performance analysis in various areas including Internet of Things, virtual emotion system, unmanned aerial vehicles, smart cities, next generation system, mobile computing and cyber security.

JALEL BEN-OTHTMAN received his Ph.D. degree from the University of Versailles, France, in 1998. He is a full professor at the University of Paris 13. His research interests are in the areas of wireless ad hoc and sensor networks, broadband wireless networks, the Internet of Things, and security in wireless networks in general and wireless sensor and ad hoc networks in particular. His work appears in highly respected international journals and conferences.

SUNGRAE CHO received the B.S. and M.S. degrees in electronics engineering from Korea University, Seoul, South Korea, in 1992 and 1994, respectively, and the Ph.D. degree in electrical and computer engineering from the Georgia Institute of Technology, Atlanta, GA, USA, in 2002. He is currently a full professor with the School of Software, Chung-Ang University, Seoul. His current research interests include wireless networking, ubiquitous computing, performance evaluation, and queuing theory.

LYNDA MOKDAD received a Ph.D. in computer science from the University of Versailles, France in 1997. She has been a full professor at the University Paris-Est, France since 2009. Her main research interests are in performance evaluation techniques and applications in wired, mobile and wireless networks and in software technologies as web services. She has published over 100 papers in highly renowned journals and conferences. She was secretary, vice chair and chair of the IEEE Communications Software committee.